Distributed Coordination of Electric Vehicles providing V2G Regulation Services

Evangelos L. Karfopoulos, *Member, IEEE*, Kostas A. Panourgias, and Nikos D. Hatziargyriou, *Fellow, IEEE*

***Abstract*—The aim of this paper is to propose a distributed electric vehicle (EV) coordination mechanism, which enables the management of the charging/discharging operation of an EV fleet, offering V2G regulation services to support system operation based on a day-ahead scheduling profile generated by an EV aggregator. Initially, a decentralized iterative algorithm is introduced to manage EV charging/discharging schedule aiming to meet the daily mobility energy requirement of an EV fleet with respect to the day-ahead schedule of the EV aggregator. Then, a droop-based control and a novel distributed regulation dispatch algorithm are developed aiming to meet the regulation dispatch signals send to the EV aggregator by the system.**

***Index Terms*—Electric vehicles (EVs), regulation service and distributed algorithm, vehicle-to-grid (V2G) demand response.**

NOMENCLATURE

$Comp_i(t)$	Compensation factor of the ith EV to account for unplanned departures.
CPA	Number of available timeslots for charging before next trip.
CP	Duration of noncommuting period.
Dci	Battery's degradation cost.
$Deg_i(t)$	Battery degradation.
d	Timeslot duration.
Efi	Efficiency of EV charger.
ExU, ExD	Expected percentage of regulation up/down capacity dispatched each hour.
ExR	Expected percentage of responsive reserve capacity dispatched each hour.
$FPi(t)$	Operational set-point of the ith EV.
Kc, Kd	Adaptive droop parameters.
Kp, Tp	Parameters of the current controller.
$L(t)$	System net load at time t.
Mci	Battery capacity of ith EV.
$MnaP_{aggr}^{for}$ $MaxaP_{aggr}^{for}$	Forecasted min/max additional power draw.
$MnAP_i(t), MxAP_i(t)$	Min/max additional power draw of ith EV.
$MnAPr_i(t)\ MaxAPr_i(t)$	Real min/max additional power draw of ith EV.
MnL, MxL	Min, max day-ahead forecasted net load.
$Mp_i(t)$	Maximum power draw of ith EV at time t.
N	Number of coordinated EVs.
$P(t)$	Energy price at time t.
$PD_i(k)$	Regulation response of the ith EV at timeslot k.
$p_i(t)$	Energy discharged due to the discharge efficiency.
$POP_{aggr}^{for}(t)$	Aggregator's energy schedule at time t.
$POP_i(t)$	Estimated operating point of ith EV.
$POP_i^{real}(k)$	Real operational set-point of the ith EV at timeslot k
$Plug_i(t)$	Dual indicator variable {0,1} defining the noncommuting hours.
$PRr(t)$	Forecasted price of spinning reserve at time t.
$PRu(t), PRd(t)$	Forecasted price of regulation up/down at time t.
$p^v(t)$	Aggregator's virtual price signal at time t.

Manuscript received January 08, 2015; revised April 17, 2015 and August 04, 2015; accepted August 12, 2015. Date of publication September 15, 2015; date of current version May 02, 2016. Paper no. TPWRS-00038-2015.

The authors are with the National Technical University of Athens, 161 21 Athens, Greece (e-mail: ekarf@power.ece.ntua.gr; kpan@mail.ntua.gr; nh@power.ece.ntua.gr).

Color versions of one or more of the figures in this paper are available online at http://ieeexplore.ieee.org.

Digital Object Identifier 10.1109/TPWRS.2015.2472957

$Ru(t), Rd(t)$	Aggregator's regulation up/down capacity.
$Rr(t)$	Aggregator's responsive reserve capacity.
$Rs(k)$	Regulation service request (%) at kth timeslot.
$Rs_{MW}(k)$	Regulation service request (MW) at kth timeslot.
$RsRP_i(t)$	Reduction in power draw available for spinning reserve of ith EV
$SOC_i(t)$	State of charge of ith EV's battery at time t.
$SOC_{min}, SOC_{max},$	$SOCin.$
$Trips_i(t)$	Low, max and plug-in initial state of charge of the ith battery.
$TSN_i(k)$	Battery consumption after ith EV travel at time t.
$X^v_{ch,i}(t)$	Number of requested timeslots for complete battery charging of ith EV at timeslot k.
$X^v_{dch,i}(t)$	Charging set-point of ith EV at time t of the vth iteration of the EV energy coordination algorithm.
ΔI_{bat}	Discharging set-point of ith EV at time t of the vth iteration of the EV energy coordination algorithm.
ΔRS	Current deviation from EV response to regulation request signal.
ΔRS	Deviation between the real and requested EV regulation power.

I. Introduction

THE aggregation and management of the battery capacity of a number of geographically dispersed electric vehicles (EVs) by a central coordinator (i.e., EV aggregator) can form a virtual storage capacity presenting specific operational constraints implied by the EV user's mobility needs and constraints, capable of offering energy and regulation services to the grid. The potential financial and network benefits from EV grid support services are analyzed in [1]–[11] considering either unidirectional and bidirectional power flow between EV and the grid. As was proven in [1]–[9], bidirectional power flow maximizes these benefits in the majority of the examined study cases, and, thus, it is also adopted here.

Existing research on the control schemes for vehicle-to-grid (V2G) regulation services provision [12] deals with droop-based [13]–[16] approaches for short-term frequency control and incentive-based approaches for longer term optimized frequency control. [17]–[21]. Droop-based approaches are used for primary frequency support of power systems aiming to contribute to the alleviation of imbalances between production and consumption. The majority of these approaches define the EVs operational set-point based purely on the system frequency deviation. Even in case of more advanced droop-based control approaches [16], where the charging needs of each individual EV are considered as a local variable, the aim is to maintain a fully charged battery without considering market prices or serving a global coordination objective, i.e. regulation request from the system, aggregator's optimal scheduling, etc.

In incentive-based approaches EV users and EV aggregators are motivated through market prices to provide regulation services in order to optimize some objective function. Optimality can be achieved either from the aggregator's ([17], [18] and [21]) or the single-vehicle's perspective [19], [18]–[20]. From the aggregator's perspective, the relatively small power of individual EVs is accumulated forming virtual energy storage. Next, the aggregator schedules the EVs charging operation over a time horizon aiming to maximize its revenues [17], [18] or minimize the global charging cost of its EV fleet [21]. In [17], the aggregator's revenues maximisation is achieved considering single vehicle optimality. Regarding the single-vehicle optimality, each individual EV defines its optimal strategy over a time horizon aiming to maximize its revenues based on its mobility constraints and charging needs, without considering other EV's behavior [19], [20]. The incentive-based approaches in [17], [19] and [21] guarantee the fulfillment of the charging energy requirements of each EV, but they consider that the charging periods are decoupled from the regulation periods. During the charging/discharging mode, the EV battery charges/discharges without being able to provide regulation services, while during the regulation mode the battery remains idle. In [12], the regulation period is elongated in order to improve the quality of the regulation service without, though, considering explicitly the revenues of the service provider.

This paper aims to introduce a distributed coordination of EV providing regulation services based on optimal day-ahead scheduling. The proposed concept combines the incentive-based concept, which defines the optimal charging/discharging operation of an EV fleet and the available regulation capacity, with the droop-based concept which enables the distributed dispatch of a regulation power signal among the EVs considering their operational status and mobility needs/constraints. The proposed concept comprises three control layers, defined here.

1) Day-ahead optimal EV scheduling algorithm: defines the optimal charging/discharging scheduling between an EV aggregator and its coordinated EVs as well as the optimal available regulation capacity aiming to maximize aggregator's profits through the provision of energy and regulation services.

2) Hourly distributed EV energy coordination algorithm to implement the EV aggregator's day-ahead scheduling: defines the operational set-point of each EV in a distributed way for each hour of the operational day considering the day-ahead scheduling profile of the EV aggregator as well as the mobility energy needs and constraints of the EV fleet.
3) Short-term distributed dispatch algorithm for V2G regulation services: defines the optimal response of each coordinated EV to a regulation power signal given the optimal set-point defined by the hourly energy coordination algorithm and the state of charge (SOC) of its battery

The first algorithm concerns the day-ahead coordination of EVs while the others are related to their coordination within the day. Particularly, the distributed energy coordination algorithm is executed in hourly base within the operational day and the dispatch algorithm for V2G regulation services runs in 5-min intervals following the regulation signal.

The contribution of this paper lies in the following aspects.

- It extends the decentralized EV coordination algorithm for tracking a given profile presented in [22] to support bidirectional power flow between EV battery and the grid. The tracked profile is derived from the day-ahead optimal EV scheduling introduced in [9].
- It evaluates the implementation of a droop-based control approach for dispatching a given regulation power signal among the coordinated EVs
- It introduces a new dispatch algorithm for distributing a given regulation power signal among the EV fleet and assesses its performance compared to the droop-based approach.
- It provides an integrated EV coordination solution for an EV aggregator for the optimal EV scheduling and dispatch coordination.

The remainder of this paper is organized as follows. Section II presents the adopted day-ahead optimal EV scheduling algorithm. Section III presents the enhanced distributed EV coordination algorithm. Section IV analyzes the two distributed dispatch algorithms for the provision of V2G regulation services. Case studies are presented and the simulation results are analyzed in Section V. A comparison analysis between the droop-based regulation algorithm and the proposed one is performed in Section VI. Finally, Section VII draws the conclusions.

II. Day-Ahead Optimal EV Scheduling

The method which enables EV aggregator to optimize energy and ancillary services scheduling, developed in [9], is applied in this study for the day-ahead scheduling. It aims to maximize aggregator's revenues (1) considering ancillary (regulation up/down and spinning reserve) services, such as peak load shaving by exploiting the bulk energy in the car batteries. The major advantage of this algorithm is that it allows for asymmetric bidding of regulation up and down and bidding of capacities of energy and services less than the available EV battery capacity.

This day-ahead optimal EV scheduling is formulated as

$$\begin{aligned} Maxf = &\sum_{t=1}^{T}\left(PRu(t)Ru(t)+PRd(t)Rd(t)+PRr(t)Rr(t)\right) \\ &+ Mk\sum_{i=1}^{N}\sum_{t=1}^{T}\left(E\left\{FP_i(t)\right\}\right) \\ &- \sum_{i=1}^{N}\sum_{t=1}^{T}\left(E\left\{FP_i(t)\right\}P(t)\right) \\ &- \sum_{i=1}^{N}\sum_{t=1}^{T}\left(Deg_i(t)\right) \end{aligned} \tag{1}$$

$$Ru(t)=\sum_{i=1}^{N}MnAP_i(t)\ and\ Rd(t)=\sum_{i=1}^{N}MxAP_i(t) \tag{2}$$

s.t.

$$h_{1,i,t}=POP_i(t)\left(1-Plug_i(t)\right)=0 \tag{3}$$

$$h_{2,i,t}=MxAP_i(t)\left(1-Plug_i(t)\right)=0 \tag{4}$$

$$h_{3,i,t}=MnAP_i(t)\left(1-Plug_i(t)\right)=0 \tag{5}$$

$$h_{4,i,t}=RsRP_i(t)\left(1-Plug_i(t)\right)=0 \tag{6}$$

$$\begin{aligned} h_{6,i}=&SOC_i(1)-\sum_{t=1}^{T}Trips_i(t) \\ &+Ef_i\sum_{t=1}^{T}\left(E\left\{FP_i(t)\right\}Comp_i(t)-\rho_i(t)\right) \\ &-Mc_i=0 \end{aligned} \tag{7}$$

$$\begin{aligned} g_{1,i,t}=&\left(MxAP_i(t)+POP_i(t)\right)Comp_i(t)Ef_i \\ &+SOC_i(t)-Mc_i\le 0 \end{aligned} \tag{8}$$

$$\begin{aligned} g_{2,i,t}=&\left(POP_i(t)-MnAP_i(t)-RsRP_i(t)-\rho_i(t)\right) \\ &Comp_i(t)Ef_i+SOC_i(t)\ge 0 \end{aligned} \tag{9}$$

$$\begin{aligned} g_{3,i}=&\sum_{\tau=1}^{t}\left(E\left\{FP_i(\tau)\right\}Comp_i(\tau)-\rho_i(\tau)\right)Ef_i \\ &+SOC_i(1)-\sum_{\tau=1}^{t}Trips_i(\tau)-Mc_i\le 0 \end{aligned} \tag{10}$$

$$\begin{aligned} g_{4,i}=&\sum_{\tau=1}^{t}\left(E\left\{FP_i(\tau)\right\}Comp_i(\tau)-\rho_i(\tau)\right)Ef_i \\ &+SOC_i(1)-\sum_{\tau=1}^{t}Trips_i(\tau)\ge 0 \end{aligned} \tag{11}$$

$$\begin{aligned} g_{5,i,t}=&\sum_{i=1}^{N}POP_i(t)-\frac{MxL-L(t)}{MxL-MnL} \\ &\sum_{i=1}^{N}\left(MP_i(t)Plug_i(t)\right)\le 0 \end{aligned} \tag{12}$$

$$\begin{aligned} g_{6,i,t}=&Deg_i(t)-\left(POP_i(t)-MnAP_i(t)ExU(t)\right. \\ &\left.-RsRP_i(t)ExR(t)\right) \\ &DC_iComp_i(t)/Ef_i\ge 0 \end{aligned} \tag{13}$$

$$g_{7,i,t}=MxAP_i(t)+POP_i(t)-MP_i(t)\le 0 \tag{14}$$

$$g_{8,i,t}=POP_i(t)-MnAP_i(t)+MP_i(t)\ge 0 \tag{15}$$

$$g_{9,i,t}=POP_i(t)-MnAP_i(t)-RsRP_i(i)+MP_i(t)\ge 0 \tag{16}$$

$$g_{10,i,t} = POP_i(t) + MP_i(t) \geq 0 \quad (17)$$
$$g_{11,i,t} = MxAP_i(t) \geq 0 \quad (18)$$
$$g_{12,i,t} = MnAP_i(t) \geq 0 \quad (19)$$
$$g_{13,i,t} = RsRP_i(t) \geq 0 \quad (20)$$
$$g_{14,i,t} = Deg_i(t) \geq 0. \quad (21)$$

The constraints in (3)–(6) express the EV operational limitation due to EV mobility. The EV batteries operational bounds are considered in (7)–(11). Equation (12) ensures that simultaneous charging does not affect the forecasted system peak load. Equation (13) refers to the battery degradation cost. The domain of definition of the decision variables is defined by (14)–(21). The term $\rho_i(\tau)$ is to account for the energy discharge from the battery due to the discharge efficiency and it is defined as $\rho_i(\tau) = Deg_i(t) \cdot (1 - Ef_i^2)/DC_i \cdot Ef_i$. A detailed analysis of the optimization problem (1)–(21) can found in [9].

III. Distributed EV Energy Coordination Algorithm Serving EV Aggregator's Day-Ahead Scheduling

The distributed EV coordination is a multiperson decision-making problem. It comprises the leader, who defines a global management strategy, and the responders, who respond to this strategy serving their own preferences. In this paper, the EV aggregator plays the role of the leader aiming to meet its market energy schedule ($POP^{\text{for}}_{\text{aggr}}$) resulting from the implementation of the day-ahead algorithm presented in Section II. Positive values of $POP^{\text{for}}_{\text{aggr}}(t)$ indicate EV aggregator's request for charging demand, while negative ones imply discharging request. Given the leader's management policy, the EVs as responders aim to fulfill their individual charging requirements considering their energy needs and mobility constraints.

The EV aggregator's management strategy is transformed into an iterative, price-based coordination control which extends the work in [22] considering bidirectional power flow by introducing an additional non-negative decision variable for the discharging operation. In each iteration k, EV aggregator generates a set of virtual price signals depending on the charging and discharging operation of the EV fleet which reflects the deviation between the aggregated EV charging/discharging profile and the day-ahead energy schedule. The EV aggregator's pricing policy yields virtual price signals to the EVs aiming to minimize the total deviation between the real EV aggregated charging/discharging profile and the optimal EV scheduling. These price signals are specified by the following formula:

$$p^v(t) = \gamma \left(\sum_{i=1}^{N} \left\{ X_{ch_i}^{v-1}(t) - X_{dch_i}^{v-1}(t) \right\} - POP_{aggr}^{for}(t) \right)$$

where

$$\gamma \in (0,1) \text{ and } X_{ch_i}^{v-1}(t), X_{dch_i}^{v-1}(t) \geq 0, \forall i, t. \quad (22)$$

The parameter γ is a positive constant which ensures the convergence of the distributed control as it is analyzed in Appendix A. The virtual prices in (22) do not reflect the EV owners' real charging cost or V2G profits, they are only defined for EV/RES coordination purposes and they are different from the energy market prices considered in Section II. For the first iteration ($v = 1$) of the proposed algorithm, the aggregator's pricing signals are determined by (22) considering that $X_{ch_i}^0(t) = X_{dch_i}^0(t) = 0$.

Based on the EV aggregator's pricing policy, each EV seeks to minimize its virtual charging cost by scheduling its operational set-points. The virtual charging cost of the EV is expressed by the following optimization problem:

$$\left[X_{ch_i}^v(t), X_{dch_i}^v(t)\right] = \min_{X_{ch_i}^v(t), X_{dch_i}^v(t)} \left\{ f_i^\nu \left(t, X_{ch_i}^v, X_{dch_i}^v, X_{ch_i}^{v-1}, X_{dch_i}^{v-1}\right) \right\}$$

where $f_i^\nu \left(t, X_{ch_i}^v, X_{dch_i}^v, X_{ch_i}^{v-1}, X_{dch_i}^{v-1}\right)$

$$= \sum_{t=1}^{24} \left\{ p^v(t) X_i^\nu(t) + \frac{1}{2} \left(X_i^v(t) - X_i^{v-1}(t) \right)^2 \right\} \quad (23)$$

and $X_i^\nu(t) = X_{ch_i}^v(t) - X_{dch_i}^v(t)$

$s.t.$

$$h_{1,i} = \sum_{t=1}^{24} \left(X_{ch_i}^v(t) \cdot Ef_i - \frac{X_{dch_i}^v(t)}{Ef_i} \right) \Delta t - \sum_{t=1}^{24} Trip_i^v(t) = 0 \quad (24)$$

$$h_{2,i,t} = (1 - Plug_i(t)) \cdot \left(X_{ch_i}^v(t) - X_{dch_i}^v(t) \right) = 0 \quad (25)$$

$$h_{3,i,t} = X_{ch_i}^v(t) \cdot X_{dch_i}^v(t) = 0 \quad (26)$$

$$g_{1,i,t} = SOCin \cdot Mci + \sum_{\tau=1}^{t} \left(X_{ch_i}^v(t) \cdot Ef_i - \frac{X_{dch_i}^v(t)}{Ef_i} \right) \Delta t - \sum_{\tau=1}^{t} Trip_i^v(\tau) - Mci \leq 0 \quad (27)$$

$$g_{2,i,t} = -SOCin \cdot Mci - \sum_{\tau=1}^{t} \left(X_{ch_i}^v(t) \cdot Ef_i - \frac{X_{dch_i}^v(t)}{Ef_i} \right) \Delta t + \sum_{\tau=1}^{t} Trip_i^v(\tau) \leq 0 \quad (28)$$

$$g_{3,i,t} = \left(X_{ch_i}^v(t) - MP_i \right), \left(X_{dch_i}^v(t) - MP_i \right) \leq 0 \quad (29)$$

$$g_{4,i,t} = X_{ch_i}^v(t), X_{dch_i}^v(t) \geq 0. \quad (30)$$

EVs respond to the EV aggregator's pricing policy by defining their optimal operational (charging/ discharging) set-points based on the optimization problem (23)–(30). The objective function in (23) comprises the virtual cost for charging ($p^v X_{chi}^v$), the virtual income from the V2G operation ($p^v X_{dchi}^v$) and the penalty term which goes to zero at convergence ($X_i^v = X_i^{v-1}$). The negative virtual income is incorporated in the optimization problem since the scope is to minimize the objective function. The implementation of the penalty term is necessary; otherwise, the aggregated EV optimal responsive profile oscillates between two states, as it is explained in [10]. The smaller the parameter γ is, the smaller is p^v with respect to (22) and, thus, the penalty term in (23) becomes more significant resulting in smaller operational

profile updates (i.e. the term $\|X_i^v - X_i^{v-1}\|^2$ becomes smaller). Thus, the application of the penalty term, which vanishes as the number of iterations of the algorithm increases by properly selecting the parameter γ, ensures the convergence of the proposed algorithm.

The constraint (24) implies that the daily battery consumption, either due to EV mobility or provision of V2G services, is fully retrieved by the end of the charging period. Constraint (25) implies that power exchange between an EV and the grid is feasible only during non-commuting hours. Equation (26) ensures that the simultaneous charging and discharging at the same timeslot t is not a feasible operation for an EV. The inequalities (27), (28) ensure that EV battery operates within acceptable limits. The parameter SOC_{in} indicates the battery's state of charge at the beginning of the charging period. The inequalities in (29) ensure that the power flow between the ith EV and the grid is in compliance with the nominal power of the charging infrastructure. The inequalities in (30) imply that the optimization variables take non-negative values.

Afterwards, the aggregator defines a new set of virtual prices for the next iteration $(\nu + 1)$ reflecting the new imbalance between the real aggregated profile $(POP_{\text{aggr}}^{\text{real}})$. and the forecasted one $(POP_{\text{aggr}}^{\text{for}})$ and anticipates the new EV fleet's response. This iterative procedure continues until equilibrium is reached.

The respective centralized EV energy coordination problem is presented in the Appendix A. Such a problem belongs to the class of quadratic, non-linear optimization ones. In quadratic problems, the increase in the computation time as a function of the number of EVs is polynomial as it is proved in [10]. Consequently, in applications with large EV fleets, the computation time is very large, making the implementation of centralized control approaches ineffective for close to real-time implementation. On the contrary, the implementation of distributed control can significantly reduce the computation time, especially when intermediate communication layers are applied as proved in [10]. In this case, the central problem is divided into several optimization subproblems which are solved simultaneously at local level.

IV. Distributed Dispatch Algorithm for V2G Regulation Services

This section presents two algorithms for defining the EV response to dispatch signals received from the system considering the regulation service capacities defined by the day ahead scheduling as well as EV user's energy needs and mobility. The first algorithm adopts the adaptive droop-based approach introduced in [16] for frequency regulation aiming to evaluate the efficiency of such approach to simultaneously serve local (i.e. EV charging needs) and global objectives (i.e. the aggregated EV responses should fulfill a specific regulation power request). It should be mentioned that the adaptive droop control introduced by [16, eq. (3)] for primary frequency regulation, it is adopted in this paper for different objective, i.e., responding to the aggregator's regulation signal. The second algorithm is a distributed control approach introduced by the authors enabling EVs to respond to regulation power signals based on their individual charging needs, their available charging period before the next trip and the aggregated EV ancillary service capacities.

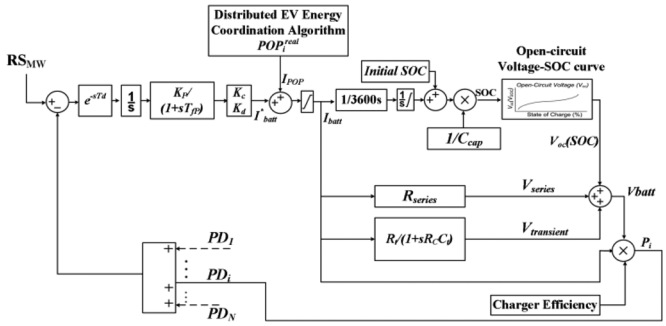

Fig. 1. Adaptive droop control based regulation dispatch algorithm.

A. Adaptive Droop-Based Regulation Dispatch Algorithm

Fig. 1 illustrates the schematic diagram of the adaptive droop-based dispatch algorithm which defines the regulation response of the ith EV (P_i) in respect to the regulation dispatch request (RS) and the charging schedule defined by the distributed EV energy coordination algorithm presented in Section III. A positive regulation signal $(RS > 0)$ results in EV charging demand increase or lower discharging rate, while negative value $(RS < 0)$ requests for less charging demand or increased discharging power.

The regulation power signal is expressed as a percentage of the reserved aggregated EV capacity for ancillary services derived by the day-ahead optimal EV scheduling as follows:

$$RS_{MW}(k) = \begin{cases} RS(k) * MnAP_{\text{aggr}}^{\text{for}}(k), & RS(k) < 0 \\ 0, & RS(k) = 0 \\ RS(k) * MxAP_{\text{aggr}}^{\text{for}}(k), & RS(k) > 0. \end{cases} \quad (31)$$

The adaptive droop control approach is based on iterative and bidirectional communication between EV and the aggregator. There is a variety of communication technologies that can be applied [23]. A delay element $e^{-T_d t}$ is considered in order to simulate the impact of communication latencies on the algorithm's convergence.

The response of each EV to the regulation signal RS, is defined by the adaptive droop-based current controller which is formulated as follows:

$$\Delta I_{bat} = K_c \frac{K_P}{(1 + sT_p)} \Delta RS_{MW},\ if\ RS_{MW} > 0 \quad (32a)$$

$$\Delta I_{bat} = K_d \frac{K_P}{(1 + sT_p)} \Delta RS_{MW},\ if\ RS_{MW} < 0 \quad (32b)$$

given that

$$K_c + K_d = 1. \quad (33)$$

1) If $\text{SOC} \leq \text{SOC}_{\min}$, then

$$K_c = 1. \quad (34)$$

2) If $\text{SOC} \geq \text{SOC}_{\max}$, then

$$K_c = 0. \quad (35)$$

3) If $\text{SOC}_{\min} \leq \text{SOC} \leq \text{SOC}_{\text{in}}$, then

$$K_c = \left(\frac{1}{2}\right)\left(1 + \sqrt{\frac{SOC - SOC_{in}}{SOC_{\min} - SOC_{in}}}\right). \quad (36)$$

4) If $\mathrm{SOC_{in}} \leq \mathrm{SOC} \leq \mathrm{SOC_{max}}$, then

$$K_c = \left(\frac{1}{2}\right)\left(1 - \sqrt{\frac{SOC - SOC_{in}}{SOC_{\max} - SOC_{in}}}\right). \quad (37)$$

From equations (34)–(37), the factor K_d can be directly defined according to the formula in (33). The resulting regulation response of each EV is added to its operational set-point defined by the EV energy coordination algorithm analyzed in Section III. The resulting current passes through the saturation block ensuring that the charging infrastructure capacity limits are not violated. The EV regulation power response is defined based on the final saturated current and the battery's characteristics, which are simulated by the Thevenin-based equivalent model [24]. R_{Series} represents the internal battery series resistance responsible for the voltage drop, while R_T and C_T are the parameters representing the battery response to transient load events. The open-circuit voltage $V_{oc}(SOC)$ is a nonlinear equation of battery's State Of Charge (SOC) [24]. C_{cap} is the battery capacity.

The adaptive droop-based regulation dispatch algorithm is a closed loop control approach. In the initial iteration, EV aggregator communicates to coordinated EVs the regulation power signal requested by the system. For the following iterations, EV aggregator communicates to EVs the difference between the real aggregated EV regulation response and the system regulation request. The algorithm terminates when the following criterion is satisfied:

$$\Delta RS_{MW} = \left|\sum_{i=1}^{N} PD_i(t) - RS_{MW}(t)\right| \leq \varepsilon, \quad i = 1, \ldots, N\ EVs. \quad (38)$$

B. Proposed Distributed Regulation Dispatch Algorithm

In the proposed regulation dispatch algorithm, the EV response is defined based on the charging energy requirements of each EV and the duration of the non-commuting period. In this respect, the participation of an EV to the regulation services in case of a charging request from the system becomes higher, as the EV energy needs increase and/or the non-commuting period shortens. On the contrary, in case of discharging request, its participation increases, when the EV has reduced energy needs and/or long non-commuting period. The proposed algorithm is an iterative process which requires the bidirectional exchange of information between the aggregator and the EVs. From the aggregator's perspective, the information communicated to the EVs is the regulation service request signal (RS_{MW} or ΔRS_{MW}, the forecasted min/max additional power drawn $(MxAP^{for}_{aggr}, MnAP^{for}_{aggr})$ and the real aggregated regulation power $(\sum_{i=1}^{N} PD_i^v)$. From the EV side, only the regulation response (PD_i of each EV in respect to the regulation request is communicated to the aggregator at each iteration. The information exchange as well as the data processing in the proposed regulation dispatch algorithm at the k-th timeslot is described by the following steps.

Step 1) The real ancillary service capacity for each individual EV is calculated as follows:

$$\begin{cases} MnAP_i^r(k) = min\left(\left|Mc_i * \frac{60}{d} - \alpha\right|, \beta_1\right) * Plug_i(k) \\ MxAP_i^r(k) = min\left(|\alpha|, \beta_2\right) * Plug_i(k) \end{cases} \quad (39)$$

$$\alpha = (1 - SOC_i(k)) * Mc_i * \frac{60}{d} - Ef_i \cdot X_i(k) \quad (40)$$

$$\beta_1 = MP_i + X_i(k)\ and\ \beta_2 = MP_i - X_i(k) \quad (41)$$

where $plug_i(k)$ is an indicator parameter denoting the mobility pattern of each EV (0 indicates commuting hours, while 1 indicates plug-in periods), a is the parameter ensuring the battery's operation within acceptable limits during timeslot k and the parameters β_1, β_2 are used for respecting the nominal power of the charging infrastructure. In the definition of the parameters α, β_1 and β_2, the optimal operational set-point of the EV $(X_i(k))$ defined by the EV coordination (23)–(30) is also considered.

Step 2) The regulation response of each EV in respect to the regulation request is defined by the following formula:

$$PD_i(k) = \begin{cases} K_i(k) * RS_{MW}(k), & RS(k) \neq 0 \\ 0, & RS(k) = 0 \end{cases} \quad (42)$$

given that

$$K_i(k) = \begin{cases} \frac{TSN_i(k)}{CPA_i(k)} \\ MxAP_i^r(k)/MxAP^{for}_{aggr}(k), & RS(k) > 0 \\ 0, & RS(k) = 0 \\ \left(1 - \frac{TSN_i(k)}{CPA_i(k)}\right) \\ MnAP_i^r(k)/MnAP^{for}_{aggr}(k), & RS(k) < 0 \end{cases} \quad (43)$$

$$TSN_i(k) = \min\left(CPA_i(k), (1 - SOC_i(k)) \cdot Mc_i \cdot \frac{60}{d}/Mpi\right) \in \mathbb{N} \quad (44)$$

$$CPA_i(k) = \sum_{\delta=k}^{\frac{60}{d}CP} \{Plug_i(\delta)\} \in \mathbb{N} \quad (45)$$

where $TSN_i(k)$ expresses the number of timeslots required for the complete charging of an EV battery, $CPA_i(k)$ defines the number of timeslots comprising the current non-commuting period (CP) i.e. the timeslots available for charging before the next trip

Step 3) Based on EV regulation responses, $PD_i(k)$, the EV aggregator calculates the deviation between the real aggregated regulation power and the requested one:

$$\Delta RS^{\nu}(k) = RS_{MW}(k) - \sum_{i=1}^{N} PD_i^{\nu}(k). \quad (46)$$

If $\Delta RS^v(k) \leq \varepsilon$ go to step 6, else continue to step 4).

Step 4) The EV regulation response in respect to the $\Delta RS^{v}(k)$ is defined by the following formula:

$$PD_i^{\nu}(k) = \begin{cases} PD_i^{\nu-1}(k) + \Delta PD_i^{\nu}(k), \\ \Delta RS^{\nu-1}(k) \neq 0 \\ 0, \Delta RS^{\nu-1}(k) = 0 \end{cases} \quad (47a)$$

where

$$\Delta PD_i^{\nu}(k) = \frac{\Delta PD_i^{\nu-1}(k)}{\sum_{i \in N_A} \Delta PD_i^{\nu-1}(k)} \Delta RS^{\nu-1}(k). \quad (47b)$$

The regulation deviation $\Delta PD_i^{v}(k)$ is bounded by the battery operational constraints $[-MnAP_i^{r}(k), MxAP_i^{r}(k)]$. In case that $\Delta PD_i^{v}(k)$ for the ith EV is saturated due to battery constraints during iteration v, then it will not participate in the regulation process for the next iterations $(> v)$ for the kth timeslot. The ith EV belongs now to the inactive subset N_I of the EV set N for the next iterations. Only EVs with unsaturated regulation deviation $\Delta PD_i^{v}(k)$ remain in the regulation process for the following iterations of kth timeslot. These EVs belong to the active subset N_A which is the complement of the subset N_I since $N = \{N_A \cup N_l\}$. In (46), for the calculation of $\Delta RS^{v}(k)$, both subsets N_A, N_l are considered. The categorization of the EVs into active and inactive sets minimizes the number of messages exchanged between EV aggregator and electric vehicles as well as it ensures convergence within a limited number of iteration as it is proved by the simulation results in Section VI.

Step 5) $\nu = \nu + 1$, return to step 3).

Step 6) When convergence is achieved

$$\left|\Delta RS^{\nu}(k) - \Delta RS^{\nu-1}(k)\right| \leq \varepsilon \quad (48)$$

the operational state of each EV is described by the following equations:

$$POP_i^{real}(k) = X_i(k) + PD_i^{\nu}(k) \quad (49a)$$

$$SOC_i(k+1) = SOC_i(k) + POP_i^{real}(k) \cdot * \frac{d}{60} / Mc_i. \quad (49b)$$

The EV response $\mathrm{PD_i^v(k)}$ defined by formulas (42) and (47) ensures that the deviation between the real aggregated regulation power and the requested one $(\Delta RS^{\mathrm{T}}v)$ vanishes as the number of iterations (v) increases. This remark is explained in detail in the Appendix B.

V. Study Case

A. EV Fleet

An EV fleet of 10 000 vehicles of types L7e and M1 is considered. The technical characteristics of the simulated EV fleet are shown in Table I. For the traffic pattern of the EV fleet the following aspects are considered.

TABLE I
EV Fleet Characteristics

	EV Number	Battery Capacity (kWh)	Consumption (kWh/km)
Type A	500	53	0,127
Type B	2000	26	0,157
Type C	2000	30	0,14
Type D	2500	16	0,125
Type E	3000	24	0,21

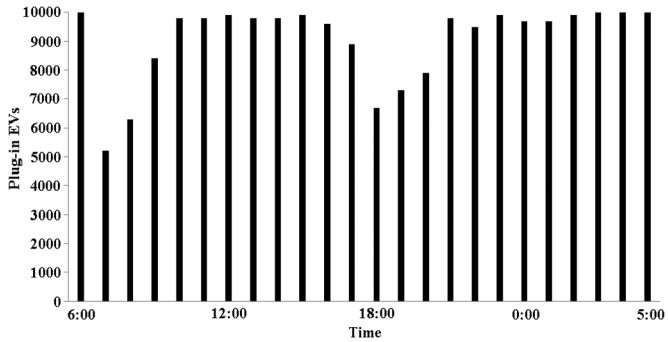

Fig. 2. Number of plug-in EV in each hour of the day.

- 06:00–09:00: It is assumed that all EVs have fully charged battery at 06:00. During this time period, it is considered that each EV makes one trip.
- 10:00–15:00: During this period it is assumed that EVs are parked and plugged-in. However, there is a random number of EVs that makes an additional trip during this period.
- 16:00–19:00: During this time period, it is considered that EVs return home and plug-in to the grid.
- 20:00–03:00: It is assumed that a random number of EVs unexpectedly departures, but all EV are plugged-in after 03:00.
- 03:00–05:00: All EVs are connected to the grid. No unexpected departure occurs.

Based on the assumed traffic patterns, the number of plugged-in EVs at each hour is illustrated in Fig. 2. Regarding the daily travelled distances (km), a normal distribution with a mean value of 40- and 5-km deviation is considered. For the arrival and departure times, normal distributions with mean values 07:30 and 17:30, with half-hour deviation, are considered, respectively. The assumption of normal distribution for the travel distance and the arrival departure time is made. The proposed EV coordination methodology however can be implemented for different traffic profiles reflecting different mobility conditions and/or EV classes (bus, tracks) without affecting the performance of the proposed methodology.

Concerning the charging infrastructures, single-phase charging stations of Mode 2 are considered according to IEC 62196-1.

B. Market Data

The simulated market data for energy and regulation services is obtained from the ERCOT market [9], as presented in Fig. 3. Regarding the retail prices, it is considered that EV users are charged at constant retail price (0.01/kWh). Furthermore, the battery degradation cost is considered at 200/kWh. Finally,

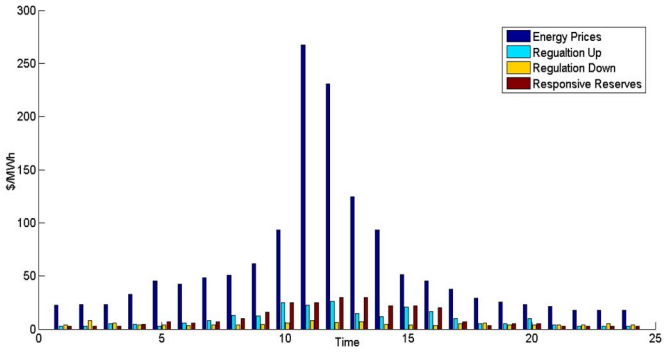

Fig. 3. Market energy price [9].

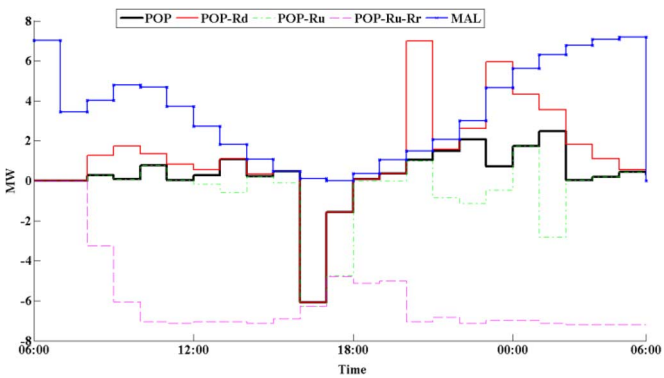

Fig. 4. Day-ahead EV scheduling.

the regulation signal exploited in the first V2G experiment of Delaware University and California's system operator is considered.[1]

VI. Results

The results of the day-ahead EV scheduling are presented in Fig. 4. The black bold line shows the energy scheduling profile of the EV aggregator considering both the forecasted charging needs of the EV fleet and the additional charging requirements resulting from the peak load shaving services. The energy scheduling profile is the tracked power profile of the distributed EV coordination algorithm. The dashed lines show the profiles of available ancillary services capacity which are exploited in the regulation dispatch algorithms. The difference between the energy profile and the ancillary services ones indicates the available reserve capacities. The blue, star-marked, continuous line indicates the maximum allowable EV load (MAL) in each hour t aiming to prevent the occurrence of a new network peak load due to the additional EV charging load. The parameter MAL is defined by the following formula:

$$MAL = \frac{MxL - L(t)}{MxL - MnL} \cdot \sum_{i=1}^{N} \left(MP_i(t) \times Plug_i(t)\right). \quad (50)$$

Figs. 5 and 6 illustrate the aggregated EV response energy profile and the EV aggregator's pricing (virtual) policy derived at the end of each iteration of the algorithm, respectively. The

[1]University of Delaware. [Online]. Available: http://www.udel.edu/V2G/Tools.html, 9/1/2013.

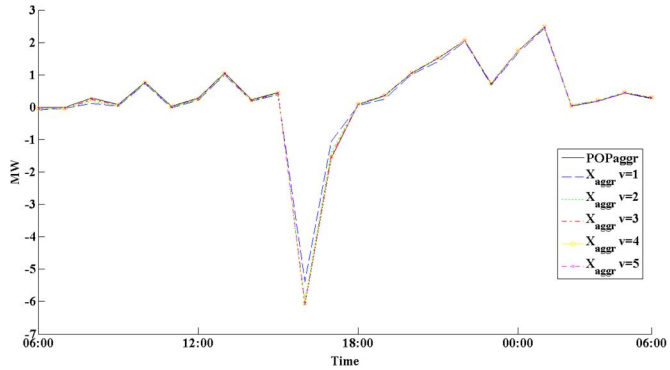

Fig. 5. Aggregated profile of EV's best response to the aggregator's pricing strategy after each iteration.

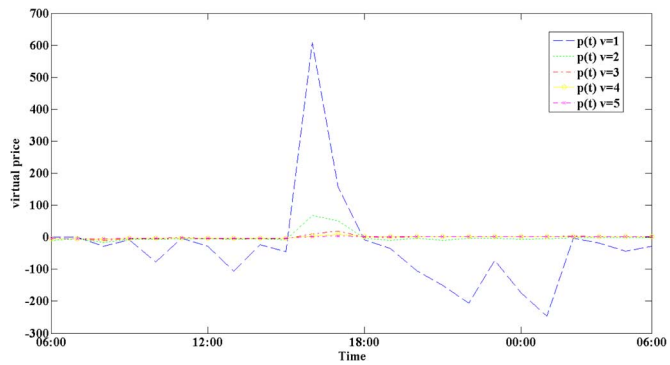

Fig. 6. EV aggregator's pricing strategy after each iteration.

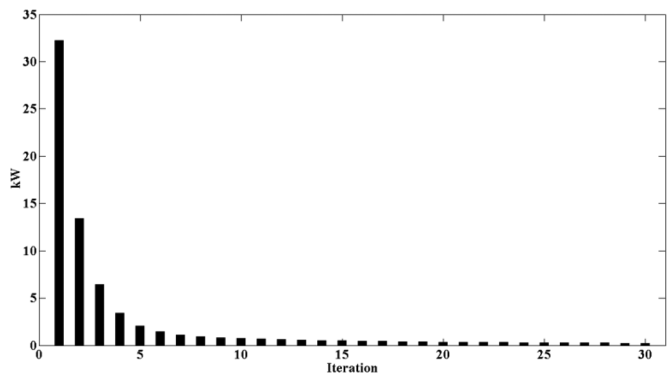

Fig. 7. RMSE of the hourly iterative EV coordination method after each iteration.

results prove the efficiency of the distributed EV coordination algorithm to track a given profile within a few computational iterations even when bidirectional power flow is considered.

Fig. 7 shows the root mean-square error (RMSE) at the end of each iteration of the distributed energy EV coordination algorithm. Even though the RMSE is high after the first iteration, it rapidly reduces after a few iterations. As the number of iterations increases, the RMSE reduction rate becomes smaller. The number of required iterations fulfilling the termination criterion defined in (38) depends on the requested accuracy ε. The tradeoff between convergence time and accuracy needs to be considered.

Fig. 8 presents indicative examples of the operation of electric vehicles with different mobility profile and energy needs. It

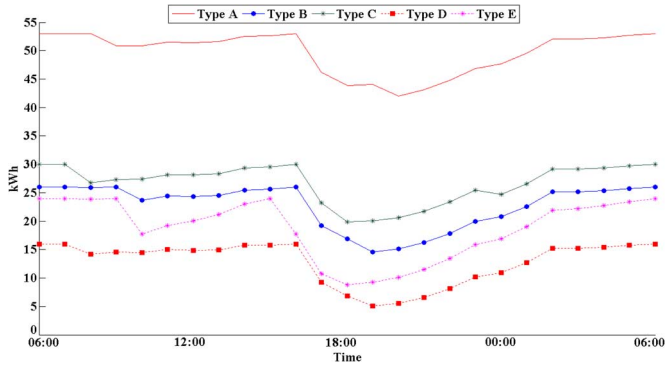

Fig. 8. Indicative examples of the battery operation of different EVs.

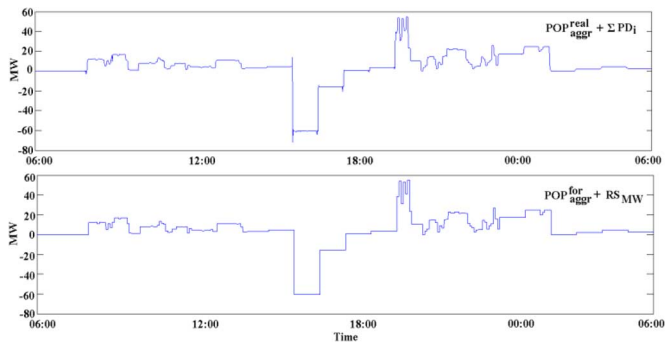

Fig. 9. Comparative simulation results between the system regulation RS and the real EV response of the adaptive droop-based dispatch algorithm ($K_p = 1$ A/MW, $T_p = 0.1$ s).

is proved that the battery's state of charge remains within acceptable operational limits throughout the examined period and it is fully charged at the end. Any increase or decrease in the state of charge indicates the respective charging or the discharging operational period. Even though different charging/discharging strategies may be adopted by each EV individually, the aggregated energy profile of the EV fleet tracks the day-ahead energy profile.

Fig. 9 shows the aggregated energy power profile of the EV fleet, considering the set-points of each EV determined by the distributed EV coordination and the regulation signal after implementation of the adaptive droop-based regulation dispatch algorithm. The upper diagram in Fig. 9 shows the real EV fleet power profile while the other presents the power profile derived from the summation of the forecasted energy scheduling profile (Fig. 4) and the regulation signal. The resulted RMSE of the droop-based regulation dispatch algorithm is 0.307 kW. For simulation purposes, the regulation interval of 5 min corresponds to 2 simulation seconds as illustrated in Fig. 10. Considering a communication delay of 100 ms, the convergence time of the adaptive droop-based control approach depends on the regulation signal modification and it varies between 0.4 and 0.8 simulation seconds or 1–2 real min.

Indicative examples of the power exchange between different types of EVs and the grid as well as the change of their battery's SOC are presented in Figs. 11 and 12. The simulation results prove that the adaptive droop-based dispatch algorithm can efficiently applied for the provision of regulation services

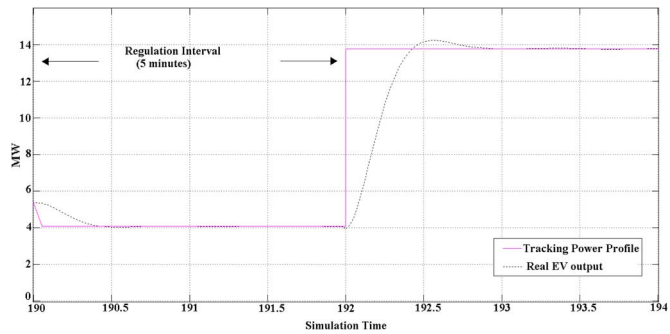

Fig. 10. Convergence time of the adaptive droop-based dispatch algorithm.

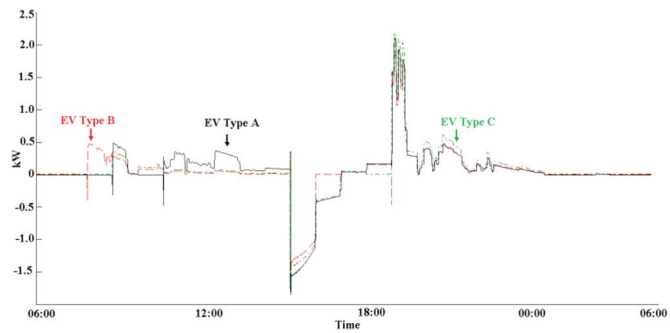

Fig. 11. Indicative examples of the power exchange between different types of EVs and the grid.

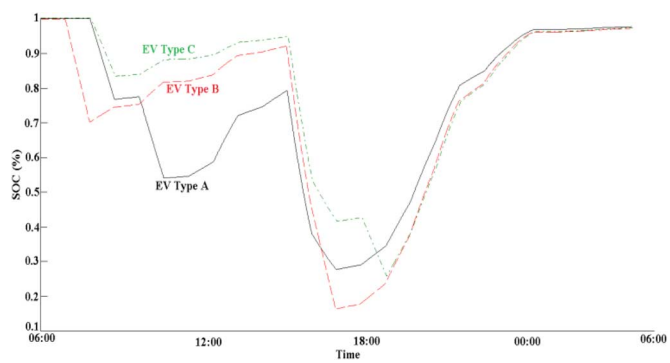

Fig. 12. SOC profile of EV batteries in case of the adaptive droop-based dispatch algorithm.

considering both local (i.e., EV travel profile, charging needs, or optimal operational set-point) and global requirements (i.e., system regulation request-RS).

The simulated results of the proposed EV regulation dispatch algorithm are shown in Figs. 13 and 14 for an indicative EV. The upper diagram presents the final 24-h EV operational profile considering the optimal scheduling set-points derived from the implementation of the distributed EV coordination algorithm and the regulation response of the EV based on the proposed distributed regulation algorithm. The lower diagram in Fig. 13 shows the SOC profile of the battery, which is maintained within acceptable bounds for the whole examined period considering travel consumption, charging/discharging optimal schedule and regulation service provision. The battery is fully charged at the end of the simulation period. Fig. 14 shows the difference between the requested regulation signal RS and the

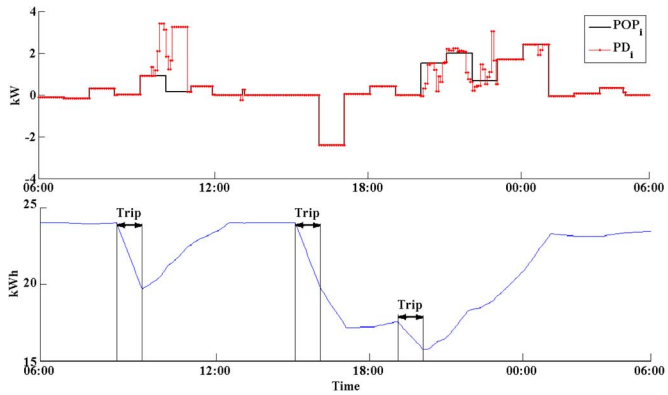

Fig. 13. Indicative simulation results of the an EV operational profile after the implementation of the proposed distributed regulation dispatch algorithm.

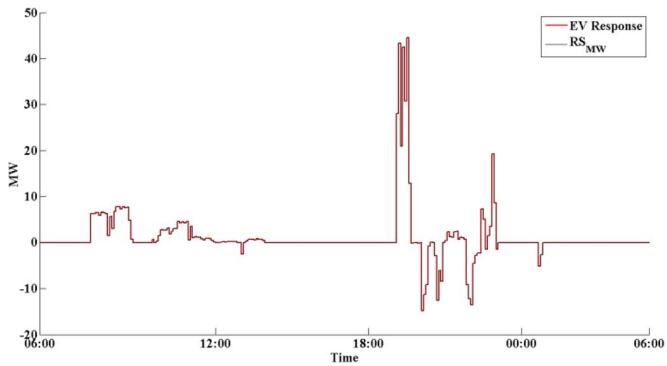

Fig. 14. Comparative results between the requested regulation signal RS and the real EV response.

real EV fleet regulation response based on the proposed distributed regulation dispatch. The resulting RMSE of the proposed regulation dispatch algorithm is 0.342 kW. The aggregated EV regulation response fulfills the system regulation requirements, which are derived based on the day-ahead energy schedule. Fig. 15 shows the number of iterations required for the convergence of the proposed EV dispatch algorithm. The algorithm converges very fast when the forecasted EV behavior of the day-ahead scheduling is close to the actual one, while the number of iterations increases slightly as the forecasting error increases. The convergence speed depends on the communication technology adopted, i.e., the data exchange delay and the number of iterations required for convergence.

VII. Comparison Analysis

This section aims to evaluate the performance of the two regulation dispatch algorithms presented in Section IV-B based on the results illustrated in Figs. 9—15. The comparative advantages of the proposed dispatch regulation algorithm over the droop-based can be grouped as follows.

- *Ease of implementation*: The convergence of droop-based control methods depends on the droop parameters (Kp, Tp). The specification of these parameters is case dependent and, thus, it requires a-priori analysis of the system behavior. On the contrary, the proposed regulation algorithm follows the "plug-n-play" concept and it does not require such parameterization.
- *Convergence Time*: As shown by the calculated RMSE values obtained by the two regulation dispatch algorithms, both dispatch solutions present similar and acceptable accuracy. However, the proposed regulation dispatch algorithm ensures very fast convergence within a few iterations, as it is proven by Fig. 15, especially in case that the nonactive subset of EVs is empty. The fast convergence is due to the definition of ΔPD_i^v in (47b). On the contrary, the droop-based control requires much more time for convergence as proven in Fig. 10 considering that the simulation time of message exchange is 100msec.
- *Charging Horizon*: In the droop-based regulation algorithm, EVs respond to the regulation signal RS_{MW} within the timeslot k based only on the current EV battery state of charge without considering its departure time. This means that two EVs with the same battery SOC but with different times of departure (i.e., different duration of the charging periods) provide identical regulation response. This may result in reduced mobility capabilities to the EV with the shortest noncommuting period. On the contrary, in the proposed regulation algorithm, both the charging needs of each EV (TSN_i) as well as their charging horizon (CPA_i) are considered resulting in a more fair allocation of the regulation signal RS_{MW}.

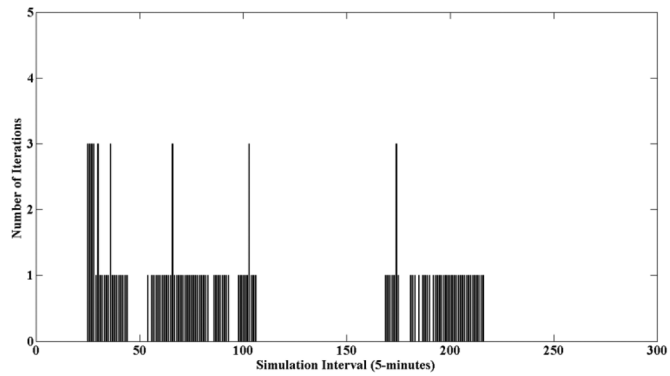

Fig. 15. Convergence iterations of the proposed EV dispatch algorithm.

VIII. Conclusion

In this paper, an integrated EV management method that can be exploited by an EV aggregator is presented. The method comprises centralized day-ahead scheduling, distributed EV coordination algorithm and distributed dispatch algorithm for V2G regulation services. The simulation results prove the efficiency of the EV coordination algorithm in managing the EVs' operation in order to meet the EV aggregator's day-ahead scheduling profile by distributed computational intelligence among the EVs. It is shown that both the adaptive droop-based approach and the proposed dispatch algorithm can fulfill successfully the dispatch objectives for V2G regulation services.

APPENDIX

Convergence of Day-Ahead Optimal Scheduling

The respective centralized problem for coordinating an EV fleet to track a given profile $D(t)$ is formulated as follows:

$$L^{v+1} = \sum_{t\in T} U\left(\sum_{i\in N} X_i^{v+1}(t) - D^{v+1}(t)\right) = \sum_{t\in T}\frac{1}{2}\left(\sum_{i\in N} X_i^{v+1}(t) - D^{v+1}(t)\right)^2$$

s.t.

$$(24)-(30) \quad \forall i \in N \tag{A1}$$

Assuming a U-function that is convex, it holds that

$$L^{v+1} \le \sum_{t\in T} U\left(\sum_{i\in N} X_i^{v}(t) - D^{v}(t)\right) - \nabla U\left(\sum_{i\in N} X_i^{v+1}(t) - D^{v+1}(t)\right)\cdot\left(\sum_{i\in N} X_i^{v}(t) - \sum_{i\in N} X_i^{v+1}(t)\right) \tag{A2}$$

given that $D^v(t) = D^{v+1}(t), \forall t \in T$

Considering that ∇U is Lipschitz, there is a Lipschitz constant $K > 0$, such that

$$|\nabla U(x) - \nabla U(y)| \le K|x-y|, \ for\ all\ x, y$$

Therefore

$$L^{v+1} \le L^v - \left\langle \nabla U\left(\sum_{i\in N} X_i^v - D^v\right) + K\left(\sum_{i\in N} X_i^{v+1} - \sum_{i\in N} X_i^v\right), \sum_{i\in N} X_i^v - \sum_{i\in N} X_i^{v+1}\right\rangle. \tag{A3}$$

According to (22), the inequality (A3) can be reformulated as follows:

$$L^{v+1} \le L^v + \frac{1}{\gamma}\sum_{i\in N}\left(p^v\cdot\left(X_i^{v+1} - X_i^v\right)\right) + K\left\|\sum_{i\in N} X_i^{v+1} - \sum_{i\in N} X_i^v\right\|^2 \tag{A4}$$

The objective function in (23) is convex since the Hessian matrix is positive semi-definite:

$$\frac{\partial f}{\partial X_{ch}^2}\frac{\partial f}{\partial X_{dch}^2} - \left(\frac{\partial f}{\partial X_{ch}\partial X_{dch}}\right)^2 > 0\, and\, \frac{\partial f}{\partial X_{ch}^2}, \frac{\partial f}{\partial X_{dch}^2} \ge 0. \tag{A5}$$

Considering that f is convex and Gateaux differentiable, from the first order optimality condition for (A1), the Euler's inequality holds:

$$\left\langle \nabla f(X^{v+1}), \sum_{i\in N} X_i - \sum_{i\in N} X_i^v\right\rangle \ge 0 \tag{A6}$$

$$\left\langle p^v + \sum_{i\in N} X_i^{v+1} - \sum_{i\in N} X_i, \sum_{i\in N} X_i - \sum_{i\in N} X_i^{v+1}\right\rangle \ge 0 \tag{A7}$$

for all $X_i \epsilon S$. Since $X_i^v \epsilon S$ then it holds that

$$\left\langle p^v + \sum_{i\in N} X_i^{v+1} - \sum_{i\in N} X_i^v, \sum_{i\in N} X_i^v - \sum_{i\in N} X_i^{v+1}\right\rangle \ge 0. \tag{A8}$$

Thus

$$\left\langle p^v, \sum_{i\in N} X_i^{v+1} - \sum_{i\in N} X_i^v\right\rangle \le -\left\|\sum_{i\in N} X_i^{v+1} - \sum_{i\in N} X_i^v\right\|^2 \tag{A9}$$

According to (A9), the inequality (A4) is modified as follows:

$$L^{v+1} \le L^v - \frac{1}{\gamma}\sum_{i\in N}\left\|X_i^{v+1} - X_i^v\right\|^2 + K\left\|\sum_{i\in N} X_i^{v+1} - \sum_{i\in N} X_i^v\right\|^2 \tag{A10}$$

Finally, according to the Cauchy-Schwarz inequality, the inequality (A10) can be as follows:

$$L^{v+1} \le L^v - \frac{1}{\gamma}\sum_{i\in N}\left\|X_i^{v+1} - X_i^v\right\|^2 + K\cdot N\sum_{i\in N}\left\|X_i^{v+1} - X_i^v\right\|^2 \tag{A11}$$

By properly selecting the parameter γ such that $\gamma < 1/(NK)$ the proposed algorithm converges since:

$$\frac{-1}{\gamma}\sum_{i\in N}\left\|X_i^{v+1} - X_i^v\right\|^2 + K\cdot N\sum_{i\in N}\left\|X_i^{v+1} - X_i^v\right\|^2 \le 0 \tag{A12}$$

and, thus, $L^{v+1} \le L^v$

If $L^{v+1} = L^v$, then $X_i^{v+1}(t) = X_i^v(t)$ and from (A7) it follows that:

$$\left\langle p^v, \sum_{i\in N} X_i - \sum_{i\in N} X_i^v\right\rangle \ge 0 \tag{A13}$$

Consequently

$$\left\langle p^v, \sum_{i\in N} X_i - \sum_{i\in N} X_i^v\right\rangle = \sum_{i\in N}\langle p^v, X_i - X_i^v\rangle \ge 0. \tag{A14}$$

This is the first-order optimality of the unconstrained optimization problem in (A1). Thus, $L^{v+1} = L^v \to X_i^{v+1} = X_i^v \to X_i^v$ is the optimal solution

Convergence of the Proposed Distributed Regulation Dispatch Algorithm

The deviation between the real aggregated regulation power and the requested one is defined by (46). For the first iteration of the algorithm and for $RS_{MW}(k) \ne 0$ it holds that

$$\Delta RS^{\nu=1}(k) = RS_{MW}(k) - \sum_{i=1}^{N} PD_i^1(k) \overset{(42)}{\Longrightarrow} \tag{B1}$$

$$\Delta RS^{\nu=1}(k) = RS_{MW}(k) - \sum_{i=1}^{N} K_i(k)\cdot RS_{MW}(k) \Longrightarrow \tag{B2}$$

$$\Delta RS^{\nu=1}(k) = \left(1 - \sum_{i=1}^{N} K_i(k)\right)\cdot RS_{MW}(k) \overset{(43)}{\Longrightarrow}. \tag{B3}$$

If $RS(k) > 0$, then

$$\Delta RS^{\nu=1}(k) = \left(1 - \sum_{i=1}^{N} \frac{TSN_i(k)}{CPA_i(k)} MxAP_i^r(k)/MxAP_{aggr}^{for}(t)\right) RS_{MW}(k). \tag{B4}$$

Considering that $\sum_{i\in N}(TSN_i(k)/CPA_i(k))MxAP_i^r(k) \leq \sum_{i\in N} MxAP_i^r(k) = MxAP_{aggr}^{for}(t)$, the regulation deviation after the first iteration ($\Delta RS^{\mathrm{T}}(v=1)$) is lower than $RS_{MW}(k)$ and depends on the ratio $TSN_i(k)/CPA_i(k)$. For any further iteration (v > 1), it holds that:

$$\Delta RS^{\nu+1}(k) = RS_{MW}(k) - \sum_{i=1}^{N} PD_i^{\nu+1}(k) \overset{(47)}{\Longrightarrow} \tag{B5}$$

$$\Delta RS^{\nu+1}(k) = RS_{MW}(k) - \sum_{i=1}^{N} \left(PD_i^{\nu}(k) + \Delta PD_i^{\nu+1}(k)\right) \tag{B6}$$

$$\Delta RS^{\nu+1}(k) = RS_{MW}(k) - \sum_{i=1}^{N} \left(PD_i^{\nu}(k) + W_{PD,i}^{v} \cdot \Delta RS^{\nu}(k)\right). \tag{B7}$$

where $W_{PD,i}^{v} = (\Delta PD_i^v(k)/\sum_{i\in N_A} \Delta PD_i^v(k))$

$$\begin{aligned}\Delta RS^{\nu+1}(k) &= RS_{MW}(k) - \sum_{i\in N} PD_i^{\nu}(k) \\ &\quad - \sum_{i\in N} W_{PD,i}^{v} \cdot \Delta RS^{\nu}(k) \\ &= \Delta RS^{\nu}(k) - \sum_{i\in N} W_{PD,i}^{v} \cdot \Delta RS^{\nu}(k) \\ &= \left(1 - \sum_{i\in N} W_{PD,i}^{v}\right) \cdot \Delta RS^{\nu}(k). \end{aligned} \tag{B8}$$

In case that $\Delta PD_i^v(k) = W_{PD,i}^v \cdot \Delta RS^v(k)$ is not saturated, the term $\sum_{i\in N} W_{PD,i}^v$ is defined as follows:

$$\sum_{i\in N} \left(\frac{PD_i^{\nu}(k)}{\sum_{i\in N} PD_i^{\nu}(k)}\right) = \frac{\sum_{i\in N} PD_i^{\nu}(k)}{\sum_{i\in N} PD_i^{\nu}(k)} = 1. \tag{B9}$$

and, thus, it holds that

$$\Delta RS^{\nu+1}(k) = 0. \tag{B10}$$

Otherwise, since $MxAP_i^r(k) < (PD_i^v(k)/\sum_{i=1}^{N} PD_i^v(k))$ it is derived that $\Delta PD_i^v(k) < W_{PD,i}^v \cdot \Delta RS^v(k)$ and it follows that

$$\Delta RS^{\nu+1}(k) < \Delta RS^{\nu}(k). \tag{B11}$$

Consequently, as the number of iterations increases the deviation between the real aggregated regulation power and the requested one is reduced even in case of saturated $\Delta PD_i^v(k)$.

A similar analysis holds for the case when $RS(k) < 0$.

REFERENCES

[1] W. Kempton and J. Tomic, "Vehicle-to-grid power fundamentals: Calculating capacity and net revenue," *J. Power Sources*, vol. 144, no. 1, pp. 268–279, Jun. 2005.

[2] W. Kempton and J. Tomic, "Vehicle-to-grid power implementation: From stabilizing the grid to supporting large-scale renewable energy," *J. Power Sources*, vol. 144, no. 1, pp. 280–294, Jun. 2005.

[3] S. De Breucker, P. Jacqmaer, K. De Brabandere, J. Driesen, and R. Belmans, "Grid power quality improvements using grid-coupled hybrid electric vehicles," in *Proc. 3rd IET Int. Conf. Power Electron., Machines and Drives*, Apr. 2006, pp. 505–509.

[4] M. Prodanovic, K. De Brabandere, J. Van den Keybus, T. Green, and J. Driesen, "Harmonic and reactive power compensation as ancillary services in inverter-based distributed generation," *IET Gener., Transm. Distrib..*, vol. 1, no. 3, pp. 432–438, May 2007.

[5] M. Caramanis and J. M. Foster, "Management of electric vehicle charging to mitigate renewable generation intermittency and distribution network congestion," in *Proc. 48th IEEE Conf. Decision and Control*, 2009, pp. 4717–4722.

[6] S. B. Peterson, J. F. Whitacre, and J. Apt, "The economics of using plug-in hybrid electric vehicle battery packs for grid storage," *J. Power Sources*, vol. 195, no. 8, pp. 2377–2384, 2010.

[7] N. Rotering and M. Ilic, "Optimal charge control of plug-in hybrid electric vehicles in deregulated electricity markets," *IEEE Trans. Power Syst.*, vol. 26, no. 3, pp. 1021–1029, Aug. 2011.

[8] M. Gallus, S. Koch, and G. Andersson, "Provision of load frequency control by phevs, controllable loads, a co-generation unit," *IEEE Trans. Ind. Electron.*, vol. 58, no. 10, pp. 4568–4582, Oct. 2011.

[9] E. Sortomme and M. A. El-Sharkawi, "Optimal scheduling of vehicle-to-grid energy and ancillary services," *IEEE Trans. Smart Grids*, vol. 3, no. 1, pp. 351–359, Mar. 2012.

[10] E. Karfopoulos and N. Hatziargyriou, "A multi-agent system for controlled charging of a large population of electric vehicles," *IEEE Trans. Power Syst.*, vol. 28, no. 4, pp. 1196–1204, Sep. 2012.

[11] M. Yilmaz and P. T. Krein, "Review of the impact of vehicle-to-grid technologies on distribution systems and utility interfaces," *IEEE Trans. Power Electron.*, vol. 28, no. 12, pp. 5673–5689, Dec. 2013.

[12] J. Lin, K. C. Leung, and V. O. K. Li, "Optimal scheduling with V2G regulation service," *IEEE J. Internet of Things*, vol. 1, no. 6, pp. 556–569, Dec. 2014.

[13] Y. Ota, H. Taniguchi, T. Nakajima, K. M. Liyanage, and A. Yokoyama, "An autonomous distributed vehicle-to-grid control of grid-connected electric vehicle," in *Proc. ICIIS*, Dec. 2009, pp. 414–418.

[14] Y. Ota, H. Taniguchi, T. Nakajima, K. M. Liyanage, J. Baba, and A. Yokoyama, "Autonomous distributed V2G (vehicle-to-grid) satisfying scheduled charging," *IEEE Trans. Smart Grid*, vol. 3, no. 1, pp. 559–564, Mar. 2012.

[15] H. Yang, C. Y. Chung, and J. Zhao, "Application of plug-in electric vehicles to frequency regulation based on distributed signal acquisition via limited communication," *IEEE Trans. Power Syst.*, vol. 28, no. 2, pp. 1017–1026, May 2013.

[16] H. Liu, Z. Hu, Y. Song, and J. Lin, "Decentralized vehicle-to-grid control for primary frequency regulation considering charging demands," *IEEE Trans. Power Syst.*, vol. 28, no. 3, Aug. 2013.

[17] S. Han, S. Han, and K. Sezaki, "Development of an optimal vehicle-to-grid aggregator for frequency regulation," *IEEE Trans. Smart Grid*, vol. 1, no. 1, pp. 65–72, Jun. 2010.

[18] S. Han, S. Han, and K. Sezaki, "Optimal control of the plug-in electric vehicles for V2G frequency regulation using quadratic programming," in *Proc. IEEE PES ISGT*, Jan. 2011, pp. 1–6.

[19] W. Shi and V. W. S. Wong, "Real-time vehicle-to-grid control algorithm under price uncertainty," in *Proc. IEEE Smart Grid Commun.*, Oct. 2011, pp. 261–266.

[20] J. Donadee and M. Ilic, "Stochastic optimization of grid to vehicle frequency regulation capacity bids," *IEEE Trans. Smart Grid*, vol. 5, no. 2, pp. 1061–1069, Mar. 2014.

[21] R. Wang, Y. Li, P. Wang, and D. Niyato, "Design of a V2G aggregator to optimize PHEV charging and frequency regulation control," in *Proc. IEEE Smart Grid Commun.*, Oct. 2013, pp. 127–132.

[22] L. Gan, U. Topcu, and S. H. Low, "Optimal decentralized protocol for electric vehicle charging," *IEEE Trans. Power Syst.*, vol. 28, no. 2, pp. 940–951, May 2013.

[23] V. C. Gungor, D. Sahin, T. Kocak, S. Ergut, C. Buccella, C. Cecati, and G. P. Hancke, "Smart grid technologies: Communication technologies and standards," *IEEE Trans. Ind. Inf.*, vol. 7, no. 4, pp. 529–539, Nov. 2011.

[24] M. Chen and G. A. Rincon-More, "Accurate electrical battery model capable predicting runtime and I–V performance," *IEEE Trans. Energy Conv.*, vol. 21, no. 2, pp. 504–511, 2006.

Evangelos L. Karfopoulos (S'05–M'15) was born in Athens, Greece, in 1982. He received the Diploma in electrical and computer engineering from the National Technical University of Athens, Athens, Greece, where he is currently working toward the Ph.D. degree.

He is also an Electrical Engineer with the Networks Development and Operation Section at the Hellenic Electricity Distribution Network Operator (HEDNO). His research interests include optimization of power system operation, distributed generation, RES and microgrids, electric vehicle management, and multi-agent system controls.

Mr Karfopoulos is a member of the Technical Chamber of Greece.

Kostas A. Panourgias was born in Athens, Greece, in 1986. He graduated from the department of Automation Engineering of the Technical Institute of Piraeus in 2008 and received the Diploma in electrical and computer engineering from the National Technical University of Athens, Athens, Greece, in 2014.

His research interests include optimization of power system operation, electric vehicle management, and automatic control systems.

Nikos D. Hatziargyriou (S'80–M'82–SM'90–F'09) was born in Athens, Greece. He received the Diploma in electrical and mechanical engineering from the National Technical University of Athens, Athens, Greece, and the M.Sc. and Ph.D. degrees in electrical power engineering from UMIST, Manchester, U.K., in 1979 and 1982, respectively.

He is a Professor with the Power Division of the Electrical and Computer Engineering Department, National Technical University of Athens, Athens, Greece. From 2007 to 2012 he was Deputy CEO of the Public Power Corporation (PPC) in Greece, responsible for Transmission and Distribution Networks, island DNO and the Center of Testing, Research and Prototyping. His research interests include smart grids, distributed energy resources, microgrids, renewable energy sources and power system security.

Prof. Hatziargyriou is the past chair of the Power System Dynamic Performance Committee and of CIGRE, SCC6, chair of the EU Advisory Council of the Technology Platform on Smart Grids.